JACS Au
AN OPEN ACCESS JOURNAL OF THE AMERICAN CHEMICAL SOCIETY

pubs.acs.org/jacsau
Article

Sorting Extrusion-Prepared Coreless Cell Membrane Vesicles of Mixed Orientations by Functional DNA Probes

Published as part of JACS Au special issue "DNA Nanotechnology for Optoelectronics and Biomedicine".

Jing Ye,[†] Fan Xu,[†] Zhihao Xu, Caiqing Yuan, Pengfei Hou, Dunkai Wu, Weifeng Han, Shufan Pan, Li Pan, Donglei Yang,* and Pengfei Wang*

Cite This: *JACS Au* 2025, 5, 1728–1737

Read Online

ACCESS | Metrics & More | Article Recommendations | Supporting Information

ABSTRACT: Cell membrane vesicles (CMVs) have been extensively used as delivery vehicles for a variety of cargos, which are generally prepared via membrane extrusion. Extruded CMVs are not necessarily to have the outer membrane facing outward due to the randomness of membrane wrapping. Nanoparticles have been used to serve as cores to direct the membrane orientation of CMVs; nevertheless, there is a lack of methods to efficiently sort coreless CMVs of desired orientations. Herein, we utilized a group of functional DNA probes to reveal the random distribution of membrane orientations of coreless CMVs after extrusion, producing either right-side-out vesicles (RSVs) or inside-out vesicles (ISVs). More importantly, DNA probes that protrude out from the outer membrane can serve as handles for efficiently sorting out RSVs from ISVs to produce vesicles with a dominant right-side-out orientation. We investigated three methods to enrich RSVs, including strand displacement reaction, photo cleavage (PC), and enzymatic cleavage. Among them, PC exhibits the highest enrichment efficiency (~93%) and RSVs purity (~85.4%), which therefore is recommended for future applications. This work revealed the mixed orientations of coreless CMVs and provided a technical platform to efficiently enrich CMVs of wanted membrane orientations that shall be useful toward a vast array of biomedical applications.

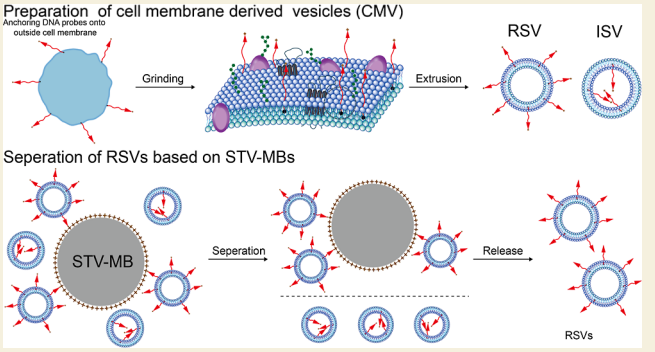

KEYWORDS: *cell membrane vesicles, extrusion, membrane orientation, DNA probes, vesicle sorting*

INTRODUCTION

With the advancement of biomedical nanotechnology, people have been enabled to more effectively detect, prevent, manage, and treat human diseases.[1−6] Inspired from nature, cell membrane vesicles (CMVs), nanosized materials prepared by isolating, disrupting, and extruding cell membranes, are emerging as one of the most promising biomimetic materials toward biomedical applications,[7,8] such as potent delivery vesicles for a variety of cargos.[8−12] Compared to other materials, CMVs have unique advantages as delivery vesicles since they inherit the surface characteristics and functional properties of parental cells, granting them superior biocompatibility, low immunogenicity, negligible toxicity, prolonged circulation, and natural targeting ability,[13,14] which therefore have found numerous applications in drug delivery,[15] biosensing,[16] and in vivo imaging.[17,18]

Red blood cells (RBC) are the most commonly used source of cellular vesicles, given their abundance in quantity and simplicity in composition.[19] Cancer CMVs also have a wide range of applications in cancer therapy because of their unique properties, including persistent existence, homotypic targeting, and antigen stimulation.[7,18] The unique properties displayed by various CMVs can largely be attributed to the complex antigenic profile present on their membranes. For example, CD47 and its analogues, which can inhibit phagocytosis and confer anti-inflammatory properties through interactions with signal regulatory protein alpha (SIRPα) expressed by macrophages, have been discovered to contribute to the in vivo survival of RBCs, cancer cells, and so on.[20−24] The principle by which cancer CMVs achieve homotypic targeting is probably through surface adhesion molecules such as N-cadherin and galectin-3.[25,26]

The preparation of CMVs employs a top-down approach, which can be broadly classified into three categories: preparation from intact cells, use of cell membrane left after the removal of

Received: December 20, 2024
Revised: March 14, 2025
Accepted: March 17, 2025
Published: March 26, 2025

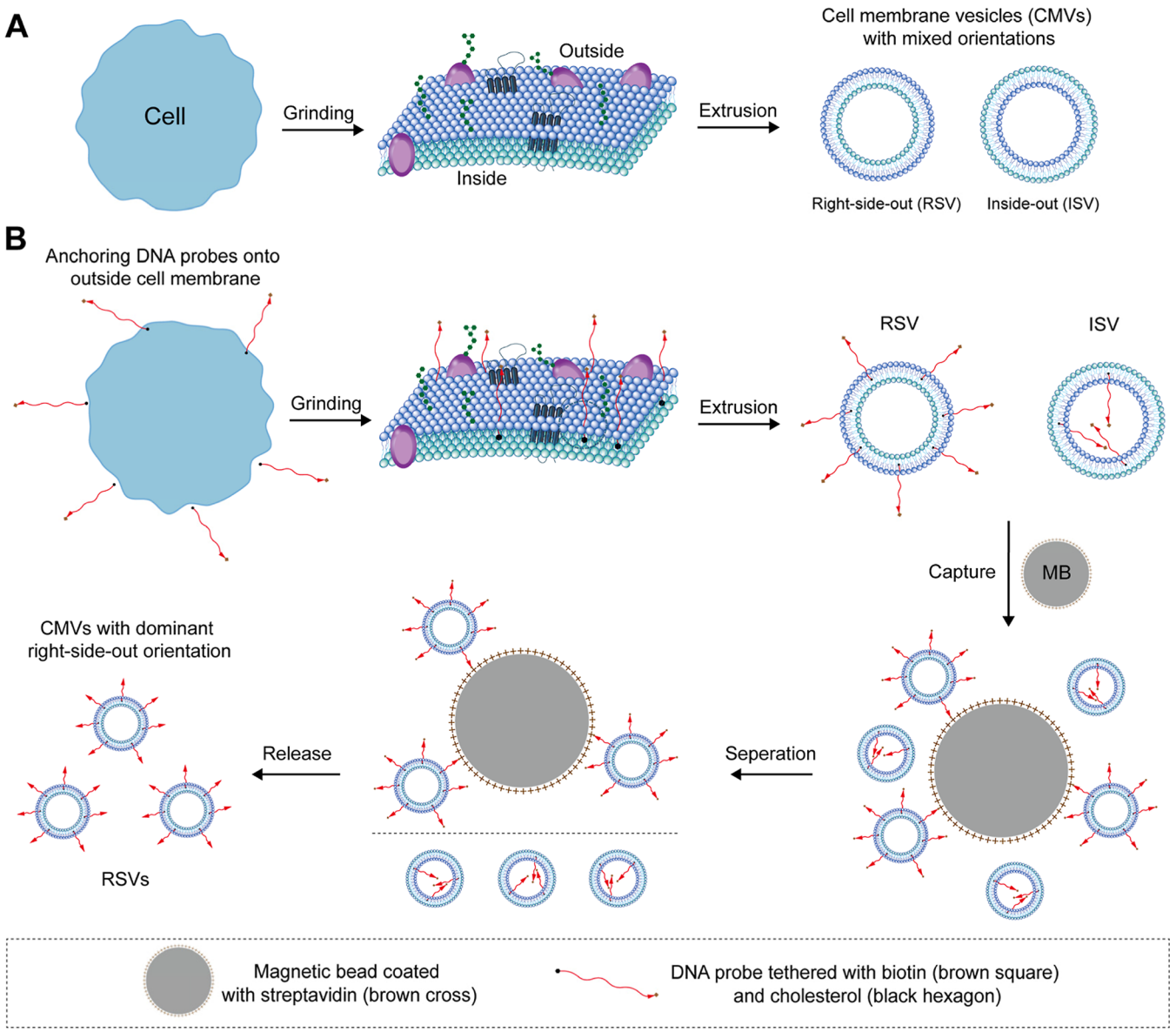

Figure 1. Functional DNA probe-enabled sorting of CMVs of mixed orientations. (A) Extrusion-prepared CMVs contain both right-side-out vesicles (RSVs) and inside-out vesicles (ISVs) due to the randomness of membrane wrapping during extrusion. (B) Working principle of using functional DNA probes to sort RSVs from ISVs. DNA probes are anchored onto the outer cell membrane before cell grinding to ensure that RSVs have DNA probes protruding out for subsequent capture and release from the magnetic beads.

cytoplasm and nucleus, or preparation of hybrid CMVs.[27] The predominant method to prepare CMVs is based on membrane extrusion through pores of defined sizes using a microextruder, which has been reported in many articles.[28,29] The complete preparation process mainly involves four steps: hypotonic treatment, dounce homogenization, continuous high-speed centrifugation, and sequential extrusion.[30] Given the randomness of membrane wrapping during extrusion, as-prepared CMVs exhibit either right-side-out orientation or inside-out orientation theoretically. CMVs primarily function as a delivery platform through the interaction between proteins or glycans on their outer membranes and the corresponding ligands.[31] Therefore, right-side-out CMVs (RSVs) are the wanted vesicles that may function well, while inside-out CMVs (ISVs) may lead to adverse reactions such as immune clearance and off-target effects due to inverted membrane orientation.[32]

A few studies have explored methodologies for characterizing the membrane orientation of CMVs with nanoparticle cores.[33] For instance, Luk et al. demonstrated that negatively charged nanoparticles could direct the formation of right-side-out CMVs, whereas positively charged nanoparticles only formed polydisperse aggregates.[34] Fan et al. developed an innovative approach to investigate membrane orientation of CNPs by employing the FRET between a 6-FAM ssDNA probe and a BHQ1 ssDNA probe quencher with a complementary sequence.[35] The investigation and regulation of membrane orientation of coreless CMVs is crucial as they have served as vital carriers for many therapeutics,[15,21,36−42] which however has rarely been investigated. Although one study has examined the orientation of membrane vesicles prepared from *Escherichia coli*,[43] there is currently a scarcity of research on the membrane orientation of coreless CMVs prepared from mammalian cells.[44] Development of such preparation methods would greatly

https://doi.org/10.1021/jacsau.4c01251
JACS Au 2025, 5, 1728−1737

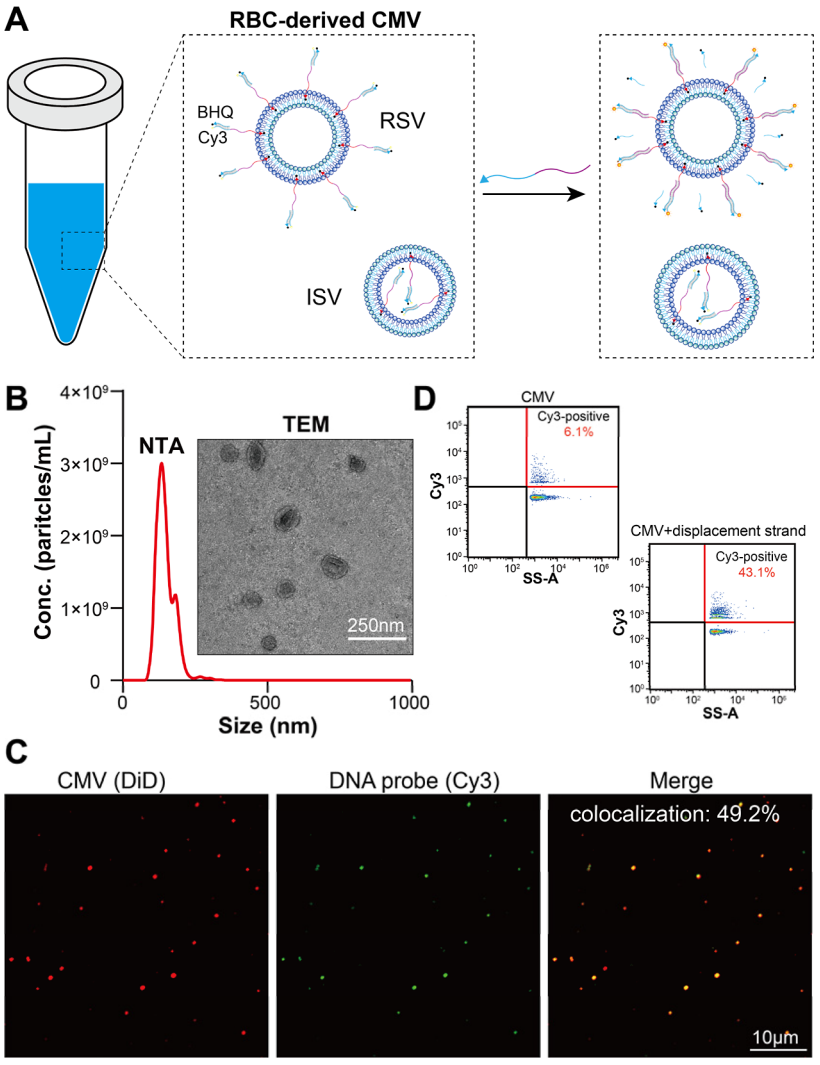

Figure 2. Revealing the mixed membrane orientations of extrusion-prepared red blood cell-derived CMVs. (A) Illustration of using DNA probes to distinguish RSVs from ISVs. (B) CMVs as measured by nanoparticle tracking analyzer (NTA) and imaged by transmission electron microscopy (TEM). (C) Confocal microscopy imaging of CMVs after adding strand displacement strand to recover the fluorescence of the anchored DNA probes. Note: only the fluorescence of DNA probes on RSVs is recovered given they are protruding out from the membrane. (D) Quantitative nanoflow cytometry analysis for CMVs with or without the addition of strand displacement strands.

contribute to enhancing the functionality of CMVs for use in biomedical applications.

In this study, we first verified that extrusion-prepared coreless CMVs exhibit mixed orientations using functional DNA probes. Amphiphilic DNA molecules, which were modified with hydrophobic groups, can stably adhere to the outer membrane of cells by integrating into the phospholipid bilayer of the cell membrane,[45−47] enabling the labeling, modification, and regulation of the cell surface. DNA probes were anchored onto the outer cell membrane prior to extrusion, serving as a handle for distinguishing RSVs from ISVs. Our study revealed that coreless CMVs extruded from RBCs membranes and cancer cell membranes exhibit mixed orientations. Then, we proposed three potent methods (strand displacement reaction (SDR), photo cleavage (PC), and enzymatic cleavage (EC)) based on functional DNA probes for sorting and enriching CMVs of wanted orientations, RSVs in this case. Through sequential reactions of functional DNA probes, we successfully enriched RSVs via binding to and then release from magnetic beads, realizing the sorting of CMVs. Additionally, we quantified the releasing efficiency of the RSVs and analyzed the purity of released RSVs. PC showed the highest releasing efficiency (~93%) and highest sorting specificity (~85.4%). We believed this study could bring important insights to draw people's attention to this critical issue of CMV membrane orientation and provide a robust technical platform to enable RSV enrichment toward various biomedical applications.

RESULTS AND DISCUSSION

Probe Design and Working Principle

The workflow of our method is illustrated in Figure 1. In principle, the extrusion-prepared coreless CMVs contain both RSVs and ISVs due to the randomness of the membrane wrapping during the extrusion process (Figure 1A). To enable distinguishing between RSVs and ISVs, cholesterol-modified DNA probes that were used (Table S1) were anchored onto cell membranes prior to grinding and extrusion to serve as indicator of the outer membrane and as a handle for magnetic beads capturing (Figure 1B). After extrusion, DNA probes protrude outward on RSVs, but protrude inward on ISVs, thus enabling

https://doi.org/10.1021/jacsau.4c01251
JACS Au 2025, 5, 1728−1737

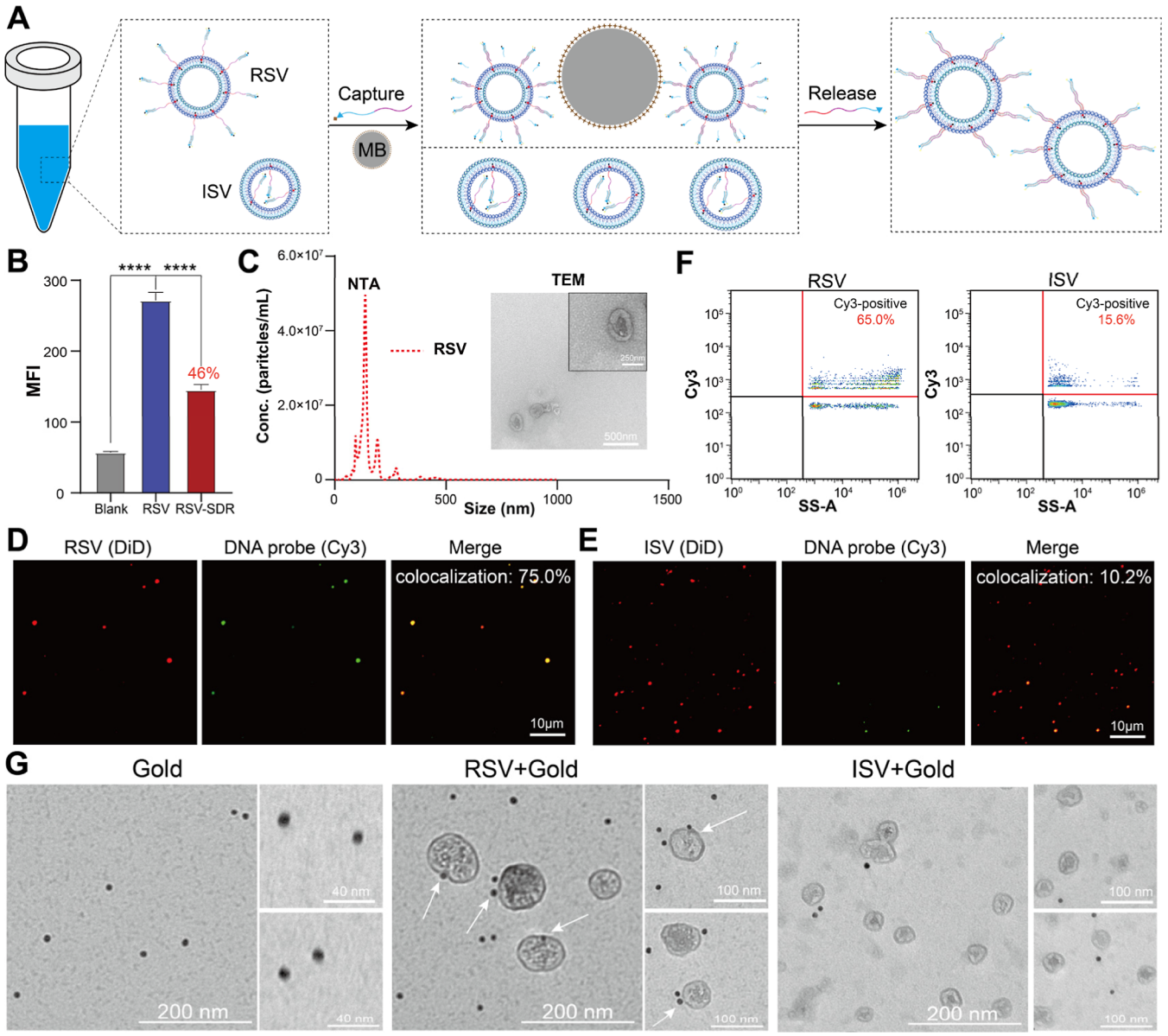

Figure 3. Sorting and validating RBC-derived CMVs. (A) Workflow of using DNA probes and magnetic beads to sort and enrich RSVs. (B) Quantitative flow cytometry analysis to reveal the binding and releasing of RSVs from magnetic beads. 46% of RSVs got released after SDR. ****$P <$ 0.0001. (C) Size distribution and morphology of sorted RSVs as measured by NTA and TEM, respectively. (D,E) Confocal microscopy imaging of RSVs and ISVs, respectively. (F) Quantitative nanoflow cytometry analysis of RSVs and ISVs. (G) Validation of RSVs and ISVs by using antibody and gold nanoparticles targeting extracellular domain of protein CD47 on the outer membrane.

discrimination between these two populations. Streptavidin-coated magnetic beads (STV-MBs) were used to specifically capture RSVs, given that RSVs bearing biotin-modified DNA probes protrude outward. RSVs were released from MBs by breaking the binding between DNA probes and MBs via various strategies. We should note that extruded CMVs may contain membranes from internal vesicles such as late endosomes. Given DNA probes can only label external membranes, CMVs originated from intracellular membranes will be characterized as ISVs, which shall not impose apparent adverse effect since RSVs are the vesicles that will be enriched for later characterizations and applications.

Extrusion-Prepared CMVs from RBCs Exhibit Mixed Orientations

Considering that RBCs are one of the main source cells for biomimetic vesicles, we first used the SDR-based sorting method to reveal whether RBC-derived CMVs exhibit mixed orientations. The workflow is illustrated in Figure 2A. First, amphiphilic DNA probes (ADP) modified with cholesterol in the 3′ end and Cy3 in the 5′ end form DNA duplex with quencher strands (QS) modified with BHQ2, which were then incubated with RBCs. CMVs were extruded using duplex-anchored membranes. Subsequently, displacement strand 1 (DS1) was added to displace the QS strand to recover the fluorescence of the anchored ADP on RSVs, given that ADP on ISVs are not accessible.

ADP and QS were mixed at equal molar concentrations to form a DNA duplex at room temperature. The change in

https://doi.org/10.1021/jacsau.4c01251
JACS Au 2025, 5, 1728−1737

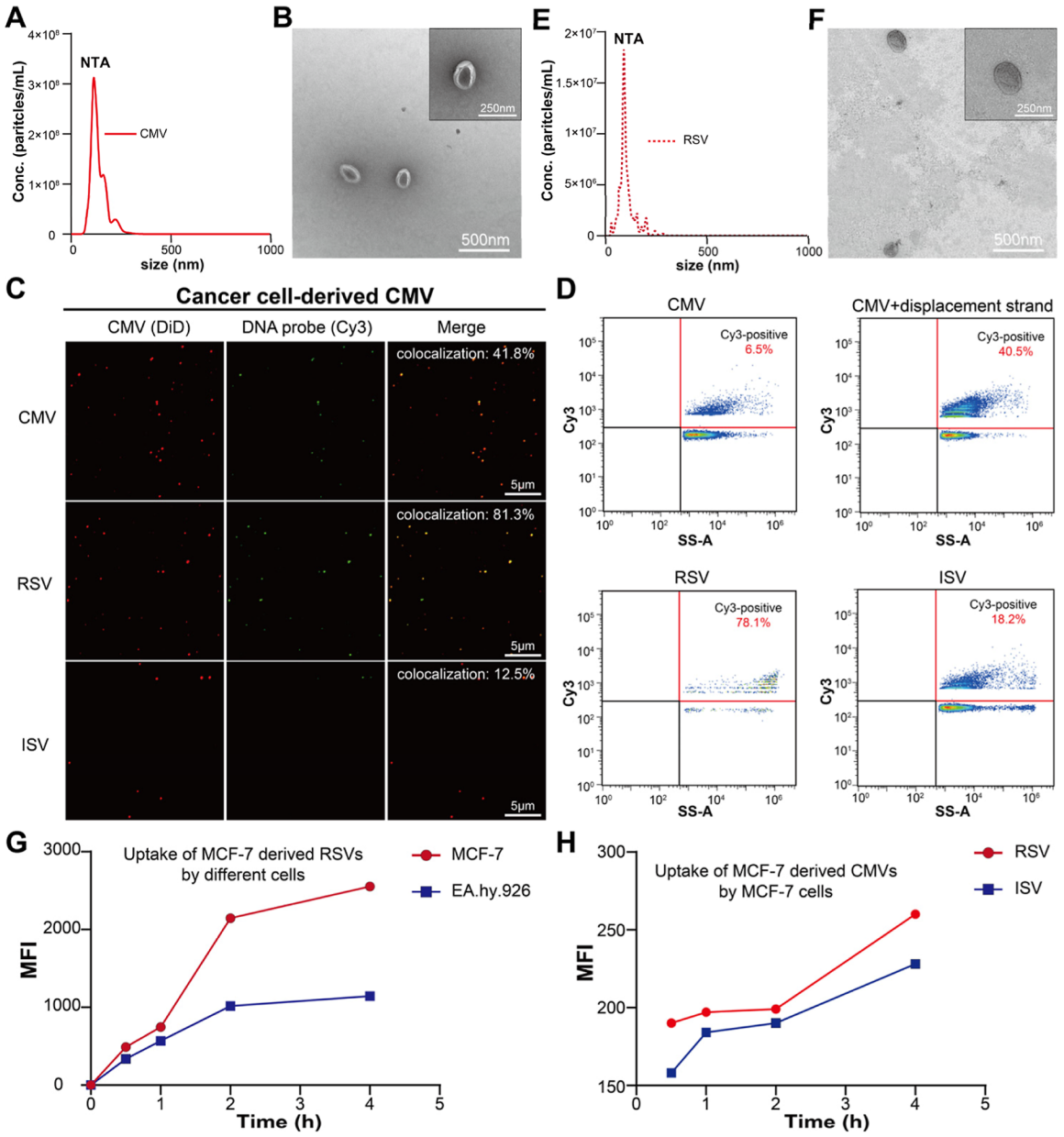

Figure 4. Sorting and validating MCF-7 cancer cell-derived CMVs. (A) Size distribution of CMVs derived from MCF-7 membrane as measured by NTA. (B) Typical saucer-like morphology of tumor CMVs as revealed by TEM. (C) Confocal microscopy imaging of CMVs of mixed orientations, RSVs, and ISVs. (D) Quantitative nanoflow cytometry analysis of CMVs, CMVs with displacement strands, and sorted RSVs, ISVs. (E) Size distribution of sorted RSVs as measured by NTA. (F) Morphology of sorted RSVs imaged by TEM. (G) Quantitative flow cytometry analysis of RSV uptake by MCF-7 and EA.hy.926 cells. (H) Quantitative flow cytometry analysis of RSV and ISV uptake by MCF-7 cells.

fluorescence intensity of Cy3 was measured before and after the assembly of the DNA duplex in the solution to assess quencher efficiency. The result showed that after forming the duplex, the fluorescence signal of the ADP significantly decreased, with the fluorescence intensity being only 0.8% of the original (Figure S1). Gel electrophoresis results indicated that the displacement strand invaded the single-stranded portion of the DNA duplex and subsequently displaced the QS in solution. Through the calculation of the gray value of the bands, it was found that when equal molar concentrations of displacement strands 1 and 2 were added, the displacement strand efficiencies of DS1 and DS2 in buffer were measured to be 95.8% and 96.5%, respectively (Figure S2).

Next, we verified the stability of the duplex and the efficiency of the SDR on CMVs. The assembled DNA duplex was anchored onto the outer membrane of RBC, and RBC-derived CMVs with a mean diameter of about 150 nm after extrusion were measured by NTA (Figure 2B). CMVs exhibited a typical saucer-like shape, as revealed by TEM (Figure 2B). The confocal microscopy imaging results are shown in Figure S3, indicating that the probes maintain a stable duplex state without Cy3 fluorescence leakage during the CMV preparation process. 49.2% of CMVs recovered the fluorescence of the anchored ADP after adding DS1 as revealed by confocal microscopy, which means the RSVs accounted for 49.2% in CMVs because only the QS facing outward on RSVs can be displaced by DS1[48] (Figures 2C and S4). Meanwhile, quantification nanoflow

https://doi.org/10.1021/jacsau.4c01251
JACS Au 2025, 5, 1728−1737

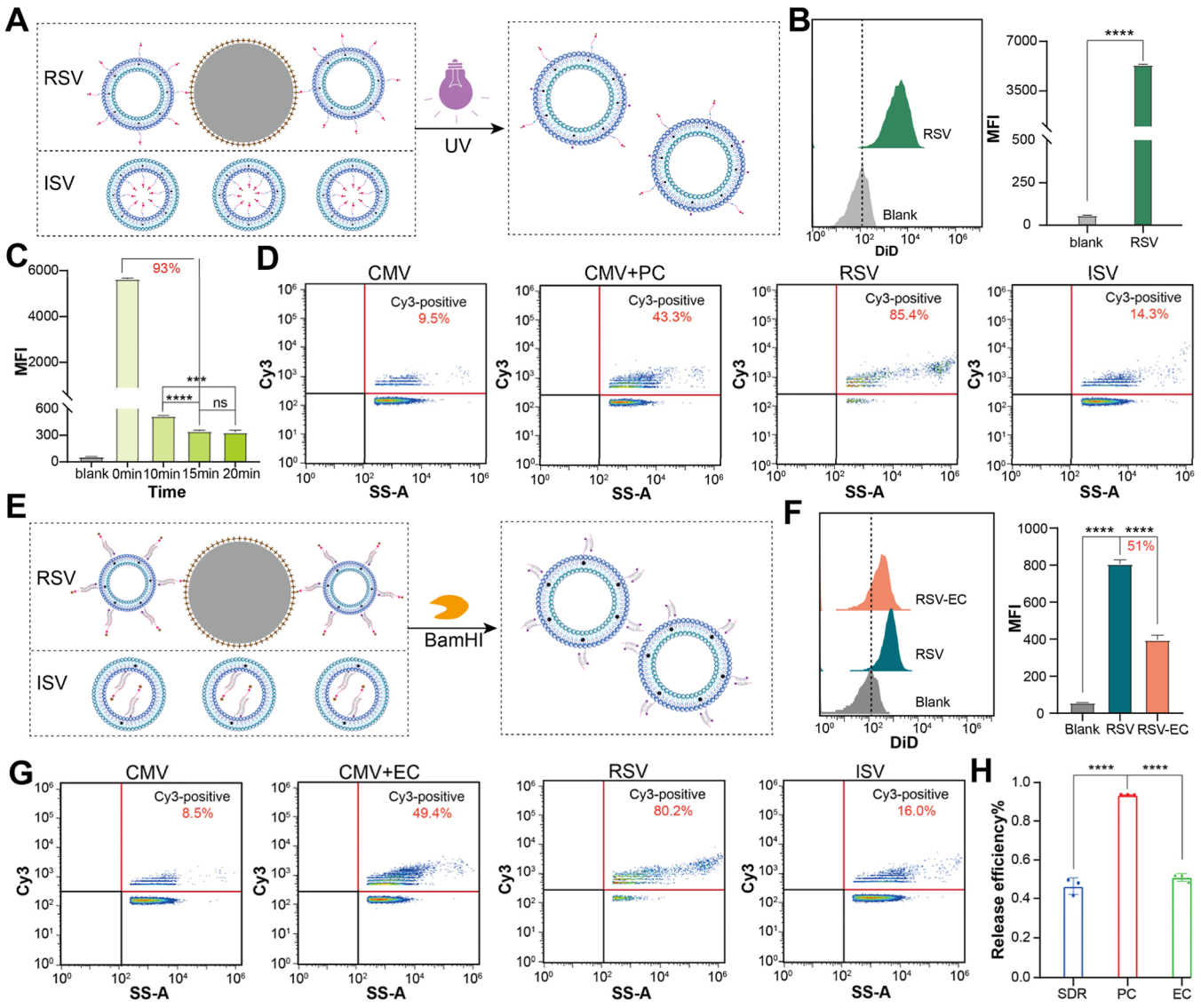

Figure 5. Enhancing CMV sorting efficiency by using PC or EC of DNA probes. (A) The schematic of sorting CMVs based on PC of DNA probes. (B) Flow cytometry analysis shows that RSVs could be captured by MBs. ****$P < 0.0001$. (C) Flow cytometry analysis indicates 15 min of UV irradiation is sufficient for inducing high releasing efficiency of RSVs. ***$P < 0.005$, ****$P < 0.0001$. (D) Nanoflow cytometry analysis of CMVs, CMVs with PC, RSVs, and ISVs. (E) The schematic of sorting CMVs based on EC of DNA probes. (F) Flow cytometry analysis of RSVs binding to MBs and releasing after EC. ****$P < 0.0001$. (G) Nanoflow cytometry analysis of CMVs, CMVs with EC, RSVs, and ISVs. (H) RSVs release efficiency for SDR, PC, and EC. ****$P < 0.0001$.

cytometry (nFCM) analysis revealed that 43.1% of CMVs recovered fluorescence with the addition of DS1 (Figure 2D). The results from the above experiments confirmed that the RBC-derived CMVs exhibit mixed orientations and the percentage of RSVs is close to 50%, which is in line with the principle of random wrapping.

Sorting and Validating RBC-Derived CMVs

After confirming that CMVs exhibit mixed orientations, we proposed a method using functional DNA probes based on SDR to sort and enrich RSVs. The workflow of distinguishing RSVs from ISVs is illustrated in Figure 3A. First, DS1 and STV-MBs were introduced to a mixed orientation CMVs sample. DS1 invaded and displaced QS protruding outward on RSVs, forming a DNA duplex with ADP. Then RSVs were enriched onto the MBs through the interaction between biotin on DS1 and streptavidin on the MBs. Second, displacement strand 2 (DS2) was added to release the RSVs from MBs, which is designed to displace DS1 and form a DNA duplex with ADP.

Quantitative flow cytometry analysis indicated the binding and release of RSVs from MBs with 46% of RSVs being released after SDR (Figures 3B and S5). NTA and TEM were performed to characterize the sorted RSVs and ISVs. The maintenance of the size and morphology of the sorted RSVs and ISVs indicated that the method would not damage the structure of CMVs (Figures 3C and S6). Having confirmed that SDR is effective for CMV sorting, we next explored the specificity of this method in enriching and releasing RSVs. Confocal microscopy imaging and nFCM analysis of RSVs and ISVs revealed that the specificity of the SDR method was not high enough to sort CMVs perfectly since the RSVs accounted for less than 80% of released RSVs (Figures 3D–F and S7). This may be due to the low efficiency of SDR in a complex environment. To validate the orientation of sorted CMVs, we conducted immunostaining experiments

https://doi.org/10.1021/jacsau.4c01251
JACS Au 2025, 5, 1728−1737

(Figure 3G). Gold-labeled anti-CD47 antibodies were used to target the extracellular domain of CD47 on the cell membrane, which could serve as an indicator of membrane orientation. As revealed, many gold nanoparticles were found attached to the external membrane of RSVs, while in contrast, very few were observed for ISVs. These data unambiguously confirmed the successful sorting of RSVs and ISVs.

Sorting and Validating Cancer Cell-Derived CMVs

We next sought to conduct sorting of CMVs derived from cancer cells, another major source of CMVs for biomedical applications. Breast cancer cell line MCF-7 was selected as the model cell line. The size of the CMVs derived from MCF-7 was measured to be approximately 140 nm by NTA (Figure 4A) and the morphology of the CMVs was imaged by TEM, which revealed a saucer-like structure (Figure 4B), confirming the successful extrusion of CMVs. We then attempted to verify the mixed orientations of MCF-7-derived CMVs following the above protocol. Confocal microscopy imaging (Figures 4C and S8) and nFCM (Figure 4D) both confirmed the coexistence of RSVs and ISVs within CMVs, with RSVs accounting for ∼ 40% of total populations. It is worth noting that the percentage of RSVs from MCF-7 cells is a bit lower than that derived from RBCs. This disparity could potentially be attributed to the purity difference of the two cell membrane samples. Unlike RBCs, MCF-7 cells contain many internal membrane vesicles (e.g., lysosomes) that cannot be labeled by DNA probes, leading to a lower percentage of the labeled cell membrane and thus a lower percentage of RSVs. After sorting CMVs by using the same SDR and magnetic beads method, RSVs were significantly enriched to ∼ 80% (Figure 4C,D). The size and morphology of enriched RSVs were characterized by NTA and TEM, respectively (Figure 4E,F and S9), which indicated that RSVs stayed intact after sorting.

The biological function of MCF-7-derived CMVs was investigated to demonstrate the superiority of RSVs with a right-side-out membrane orientation. First, MCF-7-derived RSVs were treated to two different cell lines, MCF-7 and EA.hy.926 cells. As revealed by flow cytometry (Figure 4G), RSVs exhibited significantly higher uptake efficiency into MCF-7 cells, which was expected given the well-known homotypic targeting effect. Second, MCF-7-derived RSVs and ISVs were treated to MCF-7 cells in parallel to verify whether the difference in membrane orientation affects their cell uptake efficiency (Figure 4H). As expected, MCF-7 cells showed much higher uptake efficiency of RSVs than that of ISVs, suggesting the right-side-out membrane orientation could promote its internalization into targeted cells, which is therefore a more superior delivery vehicle with pronounced application potential.

Enhancing RSV Enrichment Efficiency by Using PC and EC of DNA Probes

Although the SDR-based method showed relatively successful sorting of RSVs and ISVs, its enrichment efficiency of RSVs was not sufficiently high to meet the requirement of later practical applications. Therefore, in this section, we aimed to explore alternative strategies to achieve greater enrichment efficiency of RSVs. Specifically, PC and EC of DNA probes were investigated to release captured RSVs from magnetic beads. We chose RBC as the model cell due to its ease of operation and the high purity of the labeled membranes. The workflow of PC-based protocol is illustrated in Figure 5A. PC-strand1 (PC-S1) is modified with cholesterol in the 5′ end, with PC-linker in the middle and biotin in the 3′ end, which was anchored onto RBC outer membranes. PC-S1 anchored CMVs were extruded, followed by enrichment of RSVs through binding to MBs and release of RSVs upon ultraviolet (UV) irradiation. Gel electrophoresis confirmed the effective and rapid cleavage of the PC-linker strand after 10−30 min of UV irradiation in solution[49,50] (Figure S10). The size of the CMVs derived from the RBC was measured to be approximately 160 nm by NTA (Figure S11), which can be efficiently captured by MBs (Figure 5B). Confocal microscopy imaging revealed that after UV irradiation the fluorescence signal on the MBs decreased significantly, indicating that RSVs were successfully released from MBs (Figure S12). Furthermore, quantitative analysis by flow cytometry showed that ∼93% of RSVs could be released after 15 min of UV irradiation (Figure 5C), much higher than the SDR-based method (∼46%). The purity of the released RSVs reached ∼85.4% (Figure 5D).

The EC-based releasing protocol utilizes the cutting activity of an endonuclease, BamH1 for the enrichment of RSVs (Figure 5E). DNA probes (BamS1) modified with cholesterol in the 5′ end and biotin in the 3′ end formed DNA duplex with BamS2. The duplex contains specific double-stranded DNA sequence of ĜGATCC, which can be specifically cleavaged by BamH1.[51,52] The gel electrophoresis result proved that BamH1 was capable of recognizing specific cleavage sites and cutting the strands (Figure S13). CMVs bearing DNA probes were successfully extruded (Figure S14). RSVs were then bound to MBs and released upon enzymatic treatment (Figure 5F), achieving a releasing efficiency of ∼51%, with 80.2% of the released vehicles exhibiting right-side-out membrane orientation (Figure 5G).

In comparison, the PC-based method exhibited the highest enrichment efficiency of RSVs (Figure 5H), which was also more straightforward to operate; therefore, it shall be used for later applications. People may strive for higher purity of RSVs by further optimizing the binding conditions of CMVs and MBs, for instance by blocking nonspecific binding, by thorough washing, or by optimizing the amount of STV-MBs used.

CONCLUSIONS

In summary, we have revealed that extrusion-prepared coreless CMVs exhibit mixed orientations from both RBC and cancer cell membranes, which can be categorized into RSVs and ISVs. Given the strong correlation between the membrane orientation and target ability properties, the enrichment of RSVs is very beneficial for potential applications. For example, RSVs derived from RBCs can be utilized as delivery vehicles to enable the sustained release of drugs due to their long-circulating properties. RSVs derived from cancer cells, with their inherent homotypic targeting capability, can be employed for the targeted delivery of anticancer drugs into cancer cells of high specificity to minimize off-target delivery induced side effects. They may also be formulated into cancer vaccines to enhance immunogenicity and activate the patient's immune system, thereby achieving the goal of controlling or eliminating cancers.

We used three methods for sorting CMVs based on SDR, PC, and EC. All methods realized the sorting of CMVs, with PC emerging as the method with the highest RSV enrichment efficiency. It should be noted that it is currently unclear whether and how the integration of DNA into cell membranes may affect the orientation of as prepared CMVs. We suspect that the anchoring of DNA probes may slightly favor the formation of right-side-out vesicles given that this orientation imposes less spatial steric hindrance between probes compared to the inside-out orientation. Nevertheless, this effect was not observed in our experiments. As revealed, 40−50% of CMVs from both cell lines

https://doi.org/10.1021/jacsau.4c01251
JACS Au 2025, 5, 1728−1737

were shown to exhibit the right-side-out orientation, suggesting a relatively equal distribution of membrane orientations. In the meantime, DNA probes on the outer membrane may potentially affect the biological activity of RSVs, which demands further studies. However, DNA probes can be erased by DNase to minimize its potential influence on subsequent applications. Magnetic beads are employed for the sorting and enrichment of RSVs, which is relatively hard to scale up toward future practical applications. Potential large-scale methods may be developed in conjunction with high-performance liquid chromatography and gradient centrifugation. Nonspecific binding of ISVs to the beads or any other purification matrices shall be minimized (e.g., with harsh washing conditions) to enhance the purity of released RSVs for better biomedical performances.

In summary, we conclude that DNA can act as a powerful tool for indicating CMV orientations and for sorting CMVs of desired orientations owing to the precise and controllable nature of programmable DNA materials. This technology offers a universal platform to produce desired and homogeneous CMVs that shall find broad applications in the field of drug delivery and beyond.

■ ASSOCIATED CONTENT

Data Availability Statement

The data that support the plots and other findings of this study are either included in the Supporting Information or available from the corresponding author upon reasonable request.

Supporting Information

The Supporting Information is available free of charge at https://pubs.acs.org/doi/10.1021/jacsau.4c01251.

Verification of quenching efficiency of ADP and QS; verification of SDR and EC by gel electrophoresis; confocal microscopy imaging of DiD, Cy3, CMVs, RSVs, and ISVs; flow cytometry analysis showing RSVs can be captured by MBs; size distribution and morphology of sorted ISVs; cleavage verification of DNA probes; size distribution of DNA duplex; DNA sequences; and additional experimental details, materials, and methods (PDF)

■ AUTHOR INFORMATION

Corresponding Authors

Donglei Yang − *Institute of Molecular Medicine, Department of Laboratory Medicine, Department of Urology, Shanghai Key Laboratory for Nucleic Acid Chemistry and Nanomedicine, Renji Hospital, School of Medicine, Shanghai Jiao Tong University, Shanghai 200127, China*; Email: dongleiyang@shsmu.edu.cn

Pengfei Wang − *Institute of Molecular Medicine, Department of Laboratory Medicine, Department of Urology, Shanghai Key Laboratory for Nucleic Acid Chemistry and Nanomedicine, Renji Hospital, School of Medicine, Shanghai Jiao Tong University, Shanghai 200127, China*; orcid.org/0000-0002-3125-763X; Email: pengfei.wang@sjtu.edu.cn

Authors

Jing Ye − *Institute of Molecular Medicine, Department of Laboratory Medicine, Department of Urology, Shanghai Key Laboratory for Nucleic Acid Chemistry and Nanomedicine, Renji Hospital, School of Medicine, Shanghai Jiao Tong University, Shanghai 200127, China*

Fan Xu − *Institute of Molecular Medicine, Department of Laboratory Medicine, Department of Urology, Shanghai Key Laboratory for Nucleic Acid Chemistry and Nanomedicine, Renji Hospital, School of Medicine, Shanghai Jiao Tong University, Shanghai 200127, China*

Zhihao Xu − *Institute of Molecular Medicine, Department of Laboratory Medicine, Department of Urology, Shanghai Key Laboratory for Nucleic Acid Chemistry and Nanomedicine, Renji Hospital, School of Medicine, Shanghai Jiao Tong University, Shanghai 200127, China*

Caiqing Yuan − *Institute of Molecular Medicine, Department of Laboratory Medicine, Department of Urology, Shanghai Key Laboratory for Nucleic Acid Chemistry and Nanomedicine, Renji Hospital, School of Medicine, Shanghai Jiao Tong University, Shanghai 200127, China*

Pengfei Hou − *Institute of Molecular Medicine, Department of Laboratory Medicine, Department of Urology, Shanghai Key Laboratory for Nucleic Acid Chemistry and Nanomedicine, Renji Hospital, School of Medicine, Shanghai Jiao Tong University, Shanghai 200127, China*

Dunkai Wu − *Institute of Molecular Medicine, Department of Laboratory Medicine, Department of Urology, Shanghai Key Laboratory for Nucleic Acid Chemistry and Nanomedicine, Renji Hospital, School of Medicine, Shanghai Jiao Tong University, Shanghai 200127, China*

Weifeng Han − *Institute of Molecular Medicine, Department of Laboratory Medicine, Department of Urology, Shanghai Key Laboratory for Nucleic Acid Chemistry and Nanomedicine, Renji Hospital, School of Medicine, Shanghai Jiao Tong University, Shanghai 200127, China*

Shufan Pan − *Institute of Molecular Medicine, Department of Laboratory Medicine, Department of Urology, Shanghai Key Laboratory for Nucleic Acid Chemistry and Nanomedicine, Renji Hospital, School of Medicine, Shanghai Jiao Tong University, Shanghai 200127, China*

Li Pan − *Institute of Molecular Medicine, Department of Laboratory Medicine, Department of Urology, Shanghai Key Laboratory for Nucleic Acid Chemistry and Nanomedicine, Renji Hospital, School of Medicine, Shanghai Jiao Tong University, Shanghai 200127, China*

Complete contact information is available at: https://pubs.acs.org/10.1021/jacsau.4c01251

Author Contributions

†J.Y. and F.X. contributed equally.

Notes

The authors declare no competing financial interest.

Ethics statement: The study was approved by the Ethics Committee of Renji Hospital (KY2023-091-C), School of Medicine, Shanghai Jiao Tong University.

■ ACKNOWLEDGMENTS

The authors thank the National Key Research and Development Program of China (2021YFA0910100), the National Natural Science Foundation of China (82372349, 22304112), the Innovative Research Team of High-Level Local Universities in Shanghai (SHSMU-ZLCX20212602) for their support.

■ REFERENCES

(1) Bennett, Z. T.; Huang, G.; Dellinger, M. T.; Sumer, B. D.; Gao, J. Stepwise Ultra-pH-Sensitive Micelles Overcome a p K_a Barrier for

Systemic Lymph Node Delivery. *ACS Nano* **2024**, *18* (26), 16632−16647.
(2) Sahoo, D.; Atochina-Vasserman, E. N.; Maurya, D. S.; Arshad, M.; Chenna, S. S.; Ona, N.; Vasserman, J. A.; Ni, H.; Weissman, D.; Percec, V. The Constitutional Isomerism of One-Component Ionizable Amphiphilic Janus Dendrimers Orchestrates the Total and Targeted Activities of mRNA Delivery. *J. Am. Chem. Soc.* **2024**, *146* (6), 3627−3634.
(3) Itzhakov, R.; Hak, H.; Sadhasivam, S.; Belausov, E.; Fallik, E.; Spiegelman, Z.; Sionov, E.; Poverenov, E. Nanogel Particles Based on Modified Nucleosides and Oligosaccharides as Advanced Delivery System. *ACS Nano* **2023**, *17* (22), 23020−23031.
(4) Song, C.; Jiao, Z.; Hou, Z.; Wang, R.; Lian, C.; Xing, Y.; Luo, Q.; An, Y.; Yang, F.; Wang, Y.; Sha, X.; Ruan, Z.; Ye, Y.; Liu, Z.; Li, Z.; Yin, F. Selective Protein of Interest Degradation through the Split-and-Mix Liposome Proteolysis Targeting Chimera Approach. *J. Am. Chem. Soc.* **2023**, *145* (40), 21860−21870.
(5) Xiao, L.; Zhang, L.; Li, S.; Zhu, Y.; Yu, Q.; Liu, Z.; Qiu, M.; Li, Y.; Chen, S.; Zhou, X. Visualization and Quantification of Drug Release by GSH-Responsive Multimodal Integrated Micelles. *JACS Au* **2024**, *4* (3), 1194−1206.
(6) Wu, J.; Hu, Y.; Ye, H.; Zhang, S.; Zhu, J.; Ji, D.; Zhang, Y.; Ding, Y.; Huang, Z. One Stone Two Birds: Redox-Sensitive Colocalized Delivery of Cisplatin and Nitric Oxide through Cascade Reactions. *JACS Au* **2022**, *2* (10), 2339−2351.
(7) Meng, Q.; Zhao, Y.; Dong, C.; Liu, L.; Pan, Y.; Lai, J.; Liu, Z.; Yu, G.; Chen, X.; Rao, L. Genetically Programmable Fusion Cellular Vesicles for Cancer Immunotherapy. *Angew. Chem., Int. Ed.* **2021**, *60* (50), 26320−26326.
(8) Jiang, S.; Cai, G.; Yang, Z.; Shi, H.; Zeng, H.; Ye, Q.; Hu, Z.; Wang, Z. Biomimetic Nanovesicles as a Dual Gene Delivery System for the Synergistic Gene Therapy of Alzheimer's Disease. *ACS Nano* **2024**, *18* (18), 11753−11768.
(9) Zhang, F.; Mundaca-Uribe, R.; Askarinam, N.; Li, Z.; Gao, W.; Zhang, L.; Wang, J. Biomembrane-Functionalized Micromotors: Biocompatible Active Devices for Diverse Biomedical Applications. *Adv. Mater.* **2022**, *34* (5), 2107177.
(10) Chugh, V.; Vijaya Krishna, K.; Pandit, A. Cell Membrane-Coated Mimics: A Methodological Approach for Fabrication, Characterization for Therapeutic Applications, and Challenges for Clinical Translation. *ACS Nano* **2021**, *15* (11), 17080−17123.
(11) Pihl, J.; Clausen, T. M.; Zhou, J.; Krishnan, N.; Ørum-Madsen, M. S.; Gustavsson, T.; Dagil, R.; Daugaard, M.; Choudhary, S.; Foged, C.; Esko, J. D.; Zhang, L.; Fang, R. H.; Salanti, A. Malaria Biomimetic for Tumor Targeted Drug Delivery. *ACS Nano* **2023**, *17* (14), 13500−13509.
(12) Cao, Z.; Liu, X.; Zhang, W.; Zhang, K.; Pan, L.; Zhu, M.; Qin, H.; Zou, C.; Wang, W.; Zhang, C.; He, Y.; Lin, W.; Zhang, Y.; Han, D.; Li, M.; Gu, J. Biomimetic Macrophage Membrane-Camouflaged Nanoparticles Induce Ferroptosis by Promoting Mitochondrial Damage in Glioblastoma. *ACS Nano* **2023**, *17* (23), 23746−23760.
(13) Xu, C.; Ju, D.; Zhang, X. Cell Membrane-Derived Vesicle: A Novel Vehicle for Cancer Immunotherapy. *Front. Immunol.* **2022**, *13*, 923598.
(14) Jiang, J.; Huang, Y.; Zeng, Z.; Zhao, C. Harnessing Engineered Immune Cells and Bacteria as Drug Carriers for Cancer Immunotherapy. *ACS Nano* **2023**, *17* (2), 843−884.
(15) Wang, L.; Feng, Z.; Shen, S.; Wang, S.; Xing, J.; Huang, R.; Shen, H.; Yan, P.; Wang, J.; Zhang, W.; Liu, Y.; He, W.; Mo, R. Stabilized Cell Membrane-Derived Vesicles by Lipid Anchoring for Enhanced Drug Delivery. *ACS Nano* **2024**, *18* (41), 28081−28094.
(16) Vargas, E.; Zhang, F.; Ben Hassine, A.; Ruiz-Valdepeñas Montiel, V.; Mundaca-Uribe, R.; Nandhakumar, P.; He, P.; Guo, Z.; Zhou, Z.; Fang, R. H.; Gao, W.; Zhang, L.; Wang, J. Using Cell Membranes as Recognition Layers to Construct Ultrasensitive and Selective Bioelectronic Affinity Sensors. *J. Am. Chem. Soc.* **2022**, *144* (38), 17700−17708.
(17) Rao, L.; Cai, B.; Bu, L.-L.; Liao, Q.-Q.; Guo, S.-S.; Zhao, X.-Z.; Dong, W.-F.; Liu, W. Microfluidic Electroporation-Facilitated Synthesis of Erythrocyte Membrane-Coated Magnetic Nanoparticles for Enhanced Imaging-Guided Cancer Therapy. *ACS Nano* **2017**, *11* (4), 3496−3505.
(18) Chen, Z.; Zhao, P.; Luo, Z.; Zheng, M.; Tian, H.; Gong, P.; Gao, G.; Pan, H.; Liu, L.; Ma, A.; Cui, H.; Ma, Y.; Cai, L. Cancer Cell Membrane−Biomimetic Nanoparticles for Homologous-Targeting Dual-Modal Imaging and Photothermal Therapy. *ACS Nano* **2016**, *10* (11), 10049−10057.
(19) Nguyen, P. H. D.; Jayasinghe, M. K.; Le, A. H.; Peng, B.; Le, M. T. N. Advances in Drug Delivery Systems Based on Red Blood Cells and Their Membrane-Derived Nanoparticles. *ACS Nano* **2023**, *17* (6), 5187−5210.
(20) Sheng, S.; Jin, L.; Zhang, Y.; Sun, W.; Mei, L.; Zhu, D.; Dong, X.; Lv, F. A Twindrive Precise Delivery System of Platelet-Neutrophil Hybrid Membrane Regulates Macrophage Combined with CD47 Blocking for Postoperative Immunotherapy. *ACS Nano* **2024**, *18* (6), 4981−4992.
(21) Malhotra, S.; Dumoga, S.; Sirohi, P.; Singh, N. Red Blood Cells-Derived Vesicles for Delivery of Lipophilic Drug Camptothecin. *ACS Appl. Mater. Interfaces* **2019**, *11* (25), 22141−22151.
(22) Zhang, W.; Huang, Q.; Xiao, W.; Zhao, Y.; Pi, J.; Xu, H.; Zhao, H.; Xu, J.; Evans, C. E.; Jin, H. Advances in Anti-Tumor Treatments Targeting the CD47/SIRPα Axis. *Front. Immunol.* **2020**, *11*, 18.
(23) Zhang, X.; Fan, J.; Ju, D. Insights into CD47/SIRPα Axis-Targeting Tumor Immunotherapy. *Antib. Ther.* **2018**, *1* (2), 37−42.
(24) Wu, J.; Lu, H.; Xu, X.; Rao, L.; Ge, Y. Engineered Cellular Vesicles Displaying Glycosylated Nanobodies for Cancer Immunotherapy. *Angew. Chem., Int. Ed.* **2024**, *63* (44), No. e202404889.
(25) Feng, Q.; Yang, X.; Hao, Y.; Wang, N.; Feng, X.; Hou, L.; Zhang, Z. Cancer Cell Membrane-Biomimetic Nanoplatform for Enhanced Sonodynamic Therapy on Breast Cancer via Autophagy Regulation Strategy. *ACS Appl. Mater. Interfaces* **2019**, *11* (36), 32729−32738.
(26) Şen, O.⋯; Emanet, M.; Mazzuferi, M.; Bartolucci, M.; Catalano, F.; Prato, M.; Moscato, S.; Marino, A.; De Pasquale, D.; Pugliese, G.; Bonaccorso, F.; Pellegrini, V.; Castillo, A. E. D. R.; Petretto, A.; Ciofani, G. Microglia Polarization and Antiglioma Effects Fostered by Dual Cell Membrane-Coated Doxorubicin-Loaded Hexagonal Boron Nitride Nanoflakes. *ACS Appl. Mater. Interfaces* **2023**, *15* (50), 58260−58273.
(27) Du, Y.; Wang, H.; Yang, Y.; Zhang, J.; Huang, Y.; Fan, S.; Gu, C.; Shangguan, L.; Lin, X. Extracellular Vesicle Mimetics: Preparation from Top-Down Approaches and Biological Functions. *Adv. Healthc. Mater.* **2022**, *11* (19), 2200142.
(28) Gao, W.; Hu, C. J.; Fang, R. H.; Luk, B. T.; Su, J.; Zhang, L. Surface Functionalization of Gold Nanoparticles with Red Blood Cell Membranes. *Adv. Mater.* **2013**, *25* (26), 3549−3553.
(29) Malhotra, S.; Dumoga, S.; Sirohi, P.; Singh, N. Red Blood Cells-Derived Vesicles for Delivery of Lipophilic Drug Camptothecin. *ACS Appl. Mater. Interfaces* **2019**, *11* (25), 22141−22151.
(30) Li, C.; Zhao, Z.; Luo, Y.; Ning, T.; Liu, P.; Chen, Q.; Chu, Y.; Guo, Q.; Zhang, Y.; Zhou, W.; Chen, H.; Zhou, Z.; Wang, Y.; Su, B.; You, H.; Zhang, T.; Li, X.; Song, H.; Li, C.; Sun, T.; Jiang, C. Macrophage-Disguised Manganese Dioxide Nanoparticles for Neuroprotection by Reducing Oxidative Stress and Modulating Inflammatory Microenvironment in Acute Ischemic Stroke. *Adv. Sci.* **2021**, *8* (20), 2101526.
(31) Xia, Q.; Zhang, Y.; Li, Z.; Hou, X.; Feng, N. Red Blood Cell Membrane-Camouflaged Nanoparticles: A Novel Drug Delivery System for Antitumor Application. *Acta Pharm. Sin. B* **2019**, *9* (4), 675−689.
(32) Xie, J.; Shen, Q.; Huang, K.; Zheng, T.; Cheng, L.; Zhang, Z.; Yu, Y.; Liao, G.; Wang, X.; Li, C. Oriented Assembly of Cell-Mimicking Nanoparticles *via* a Molecular Affinity Strategy for Targeted Drug Delivery. *ACS Nano* **2019**, *13* (5), 5268−5277.
(33) Hu, C.-M. J.; Fang, R. H.; Luk, B. T.; Chen, K. N. H.; Carpenter, C.; Gao, W.; Zhang, K.; Zhang, L. "Marker-of-Self" Functionalization of Nanoscale Particles through a Top-down Cellular Membrane Coating Approach. *Nanoscale* **2013**, *5* (7), 2664−2668.
(34) Luk, B. T.; Jack Hu, C. M.; Fang, R. H.; Dehaini, D.; Carpenter, C.; Gao, W.; Zhang, L.; Dehaini, D.; Carpenter, C. W.; Carpenter, C.

https://doi.org/10.1021/jacsau.4c01251
JACS Au 2025, 5, 1728−1737

W.; Gao, W.; Gao, W.; Zhang, L.; Zhang, L. Interfacial Interactions between Natural RBC Membranes and Synthetic Polymeric Nanoparticles. *Nanoscale* **2013**, *6* (5), 2730−2737.
(35) Fan, Z.; Zhou, H.; Li, P. Y.; Speer, J. E.; Cheng, H. Structural Elucidation of Cell Membrane-Derived Nanoparticles Using Molecular Probes. *J. Mater. Chem. B* **2014**, *2*, 8231−8238.
(36) Zhang, C.; Tang, S.; Wang, M.; Li, L.; Li, J.; Wang, D.; Mi, X.; Zhang, Y.; Tan, X.; Yue, S. "Triple-Punch" Strategy Exosome-Mimetic Nanovesicles for Triple Negative Breast Cancer Therapy. *ACS Nano* **2024**, *18* (7), 5470−5482.
(37) Zhang, L.; Li, Z.; Wang, F.; Chen, Q.; Zu, M.; Li, X.; Wan, J.; Yao, X.; Lou, X.; Shi, Y.; Sheng, Y.; Wang, M.; Yang, J.; Wang, X.; Qin, Z.; Ji, T. Integrin-Enriched Membrane Nanocarrier for the Specific Delivery of RGD-modified Relaxin Analog to Inhibit Pancreatic Cancer Liver Metastasis through Reversing Hepatic Stellate Cell Activation. *Adv. Funct. Mater.* **2022**, *32* (47), 2208404.
(38) Wu, H.; Jiang, X.; Li, Y.; Zhou, Y.; Zhang, T.; Zhi, P.; Gao, J. Engineering Stem Cell Derived Biomimetic Vesicles for Versatility and Effective Targeted Delivery. *Adv. Funct. Mater.* **2020**, *30* (49), 2006169.
(39) Jang, Y.; Cho, Y. S.; Kim, A.; Zhou, X.; Kim, Y.; Wan, Z.; Moon, J. J.; Park, H. CXCR4-Targeted Macrophage-Derived Biomimetic Hybrid Vesicle Nanoplatform for Enhanced Cancer Therapy through Codelivery of Manganese and Doxorubicin. *ACS Appl. Mater. Interfaces* **2024**, *16* (14), 17129−17144.
(40) Chen, X.; Ling, X.; Xia, J.; Zhu, Y.; Zhang, L.; He, Y.; Wang, A.; Gu, G.; Yin, B.; Wang, J. Mature Dendritic Cell-Derived Dendrosomes Swallow Oxaliplatin-Loaded Nanoparticles to Boost Immunogenic Chemotherapy and Tumor Antigen-Specific Immunotherapy. *Bioact. Mater.* **2022**, *15*, 15−28.
(41) Chai, Z.; Ran, D.; Lu, L.; Zhan, C.; Ruan, H.; Hu, X.; Xie, C.; Jiang, K.; Li, J.; Zhou, J.; Wang, J.; Zhang, Y.; Fang, R. H.; Zhang, L.; Lu, W. Ligand-Modified Cell Membrane Enables the Targeted Delivery of Drug Nanocrystals to Glioma. *ACS Nano* **2019**, *13* (5), 5591−5601.
(42) Zhang, X.; Angsantikul, P.; Ying, M.; Zhuang, J.; Zhang, Q.; Wei, X.; Jiang, Y.; Zhang, Y.; Dehaini, D.; Chen, M.; Chen, Y.; Gao, W.; Fang, R. H.; Zhang, L. Remote Loading of Small-Molecule Therapeutics into Cholesterol-Enriched Cell-Membrane-Derived Vesicles. *Angew. Chem. Int. Ed* **2017**, *56* (45), 14075−14079.
(43) Futai, M. Orientation of Membrane Vesicles fromEscherichia Coli Prepared by Different Procedures. *J. Membr. Biol.* **1974**, *15* (1), 15−28.
(44) Steck, T. L.; Weinstein, R. S.; Straus, J. H.; Wallach, D. F. H. Inside-Out Red Cell Membrane Vesicles: Preparation and Purification. *Science* **1970**, *168* (3928), 255−257.
(45) Li, J.; Xun, K.; Pei, K.; Liu, X.; Peng, X.; Du, Y.; Qiu, L.; Tan, W. Cell-Membrane-Anchored DNA Nanoplatform for Programming Cellular Interactions. *J. Am. Chem. Soc.* **2019**, *141* (45), 18013−18020.
(46) Du, Y.; Lyu, Y.; Lin, J.; Ma, C.; Zhang, Q.; Zhang, Y.; Qiu, L.; Tan, W. Membrane-Anchored DNA Nanojunctions Enable Closer Antigen-Presenting Cell−T-Cell Contact in Elevated T-Cell Receptor Triggering. *Nat. Nanotechnol.* **2023**, *18* (7), 818−827.
(47) Chen, H.; Ding, Q.; Li, L.; Wei, P.; Niu, Z.; Kong, T.; Fu, P.; Wang, Y.; Li, J.; Wang, K.; Zheng, J. Extracellular Vesicle Spherical Nucleic Acids. *JACS Au* **2024**, *4* (6), 2381−2392.
(48) Liu, H.; Liu, S.; Xiao, Y.; Song, W.; Li, H.; Ho, L. W. C.; Shen, Z.; Choi, C. H. J. A pH-Reversible Fluorescent Probe for *in Situ* Imaging of Extracellular Vesicles and Their Secretion from Living Cells. *Nano Lett.* **2021**, *21* (21), 9224−9232.
(49) Diao, N.; Hou, J.; Peng, X.; Wang, Y.; He, A.; Gao, H.; Yang, L.; Guo, P.; Wang, J.; Han, D. Multiplexed and Quantitative Imaging of Live-Cell Membrane Proteins by a Precise and Controllable DNA-Encoded Amplification Reaction. *Angew. Chem., Int. Ed.* **2024**, *63* (40), No. e202406330.
(50) Yi, D.; Zhao, H.; Zhao, J.; Li, L. Modular Engineering of DNAzyme-Based Sensors for Spatioselective Imaging of Metal Ions in Mitochondria. *J. Am. Chem. Soc.* **2023**, *145* (3), 1678−1685.
(51) Daniel, B.; Yost, K. E.; Hsiung, S.; Sandor, K.; Xia, Y.; Qi, Y.; Hiam-Galvez, K. J.; Black, M.; Raposo, C. J.; Shi, Q.; Meier, S. L.; Belk, J. A.; Giles, J. R.; Wherry, E. J.; Chang, H. Y.; Egawa, T.; Satpathy, A. T. Divergent Clonal Differentiation Trajectories of T Cell Exhaustion. *Nat. Immunol.* **2022**, *23* (11), 1614−1627.
(52) Naderi, J.; Magalhaes, A. P.; Kibar, G.; Stik, G.; Zhang, Y.; Mackowiak, S. D.; Wieler, H. M.; Rossi, F.; Buschow, R.; Christou-Kent, M.; Alcoverro-Bertran, M.; Graf, T.; Vingron, M.; Hnisz, D. An Activity-Specificity Trade-off Encoded in Human Transcription Factors. *Nat. Cell Biol.* **2024**, *26* (8), 1309−1321.

https://doi.org/10.1021/jacsau.4c01251
JACS Au 2025, 5, 1728−1737